



HAL
open science

The first ET salt with a metal complex anion containing a selenocyanate ligand, $(\text{ET})_2\text{TlHg}(\text{SeCN})_4$: synthesis, structure and properties

L. Buravov, N. Kushch, V. Laukhin, A. Khomenko, E. Yagubskii, M. Kartsovnik, A. Kovalev, L. Rozenberg, R. Shibaeva, M. Tanatar, et al.

► To cite this version:

L. Buravov, N. Kushch, V. Laukhin, A. Khomenko, E. Yagubskii, et al.. The first ET salt with a metal complex anion containing a selenocyanate ligand, $(\text{ET})_2\text{TlHg}(\text{SeCN})_4$: synthesis, structure and properties. *Journal de Physique I*, 1994, 4 (3), pp.441-451. 10.1051/jp1:1994150 . jpa-00246919

HAL Id: jpa-00246919

<https://hal.science/jpa-00246919v1>

Submitted on 4 Feb 2008

HAL is a multi-disciplinary open access archive for the deposit and dissemination of scientific research documents, whether they are published or not. The documents may come from teaching and research institutions in France or abroad, or from public or private research centers.

L'archive ouverte pluridisciplinaire **HAL**, est destinée au dépôt et à la diffusion de documents scientifiques de niveau recherche, publiés ou non, émanant des établissements d'enseignement et de recherche français ou étrangers, des laboratoires publics ou privés.

Classification
Physics Abstracts
72.15G — 72.15N

The first ET salt with a metal complex anion containing a selenocyanate ligand, $(\text{ET})_2\text{TIHg}(\text{SeCN})_4$: synthesis, structure and properties

L. I. Buravov ⁽¹⁾, N. D. Kushch ⁽¹⁾, V. N. Laukhin ⁽¹⁾, A. G. Khomenko ⁽¹⁾,
E. B. Yagubskii ⁽¹⁾, M. V. Kartsovnik ⁽²⁾, A. E. Kovalev ⁽²⁾, L. P. Rozenberg ⁽²⁾,
R. P. Shibaeva ⁽²⁾, M. A. Tanatar ⁽³⁾, V. S. Yefanov ⁽³⁾, V. V. Dyakin ⁽³⁾
and V. A. Bondarenko ⁽⁴⁾

⁽¹⁾ Institute of Chemical Physics in Chernogolovka, Russian Academy of Science, Chernogolovka, 142432, Russia

⁽²⁾ Institute of Solid State Physics, Russian Academy of Science, Chernogolovka, 142432, Russia

⁽³⁾ Institute of Surface Chemistry, Ukrainian Academy of Sciences, Kiev, Ukraine

⁽⁴⁾ Institute of Semiconductors, Ukrainian Academy of Sciences, Kiev, Ukraine

(Received 8 October 1993, accepted 25 November 1993)

Abstract. — Synthesis of the first ET salt with a metal complex anion containing a selenocyanate ligand, $\alpha\text{-(ET)}_2\text{TIHg}(\text{SeCN})_4$, and its structure are reported. The temperature dependence of conductivity and thermopower in various crystallographic directions and the Shubnikov-de Haase oscillations have been studied. Distinctions of the bond length distributions in three crystallographically independent ET have been found, which may result in some charge localization in the radical-cation layer. A detailed comparison of the structure and properties of the compound obtained to its thiocyanate analog has been performed. It has been shown that in the $\alpha\text{-(ET)}_2\text{TIHg}(\text{SeCN})_4$ salt there is no low-temperature phase transition characteristic of the $\alpha\text{-(ET)}_2\text{MHg}(\text{SCN})_4$ compounds with $M = \text{K}, \text{Tl}$ and Rb .

Introduction.

Radical-cation salts of bis(ethylenedithio)tetrathiafulvalene (ET) with polymer metal complex anions $[\text{MHg}(\text{SCN})_4]^-$ have a layer-like cation-anion structure and peculiar physical properties. One-charge cation M entering the composition of the $[\text{MHg}(\text{SCN})_4]^-$ anion produces considerable effect on the structure and electroconducting properties of these ET salts. In the case of M with relatively close ion radii (K, NH_4 , Tl, Rb) isostructural salts of the $(\text{ET})_2\text{MHg}(\text{SCN})_4$ composition are formed. They are quasi two-dimensional metals either with a superconducting transition at $0.8 \div 1.4$ K ($M = \text{NH}_4$) [1, 2] or with a phase transition at $8 \div 10$ K ($M = \text{K}, \text{Tl}, \text{Rb}$ [3-5]), which is likely to be associated with the formation of

magnetic order (spin density wave, SDW) [6]. The latter exhibit some unexpected properties in strong magnetic fields [3, 4, 6-12]. In particular, giant angular oscillations of magnetoresistance and Shubnikov-de Haase oscillations have been observed that are very useful in providing quantitative information about their Fermi surface. It has been recently shown that the salt with $M = K$ exhibits a weak superconductivity below 300 mK [13].

Using alkali metals with an extremely small (Li) or large (Cs) ion radius as a cation M leads to the formation of dielectric salts at low temperature, which are not isostructural with α -(ET)₂MHg(SCN)₄ ($M = K, NH_4, Tl, Rb$), the lithium salt having different stoichiometry, (ET)₃Li_{0.5}Hg(SCN)₄.H₂O [14].

The properties of ET salts with the MHg(SCN)₄ anion have been modified so far *via* variations of M . However, the specificity of this complex anion allows the substitution of a thiocyanate ligand for a selenocyanate one. Such a substitution must not affect the anion nature much, since selenocyanates are often isostructural with thiocyanates. At the same time, the procedure may cause alterations of the physical properties like in the series of isostructural (ET)₂MHg(SCN)₄ salts with different M .

In the present paper we report the synthesis of the first ET salt with a metal complex anion containing a selenocyanate ligand, (ET)₂TlHg(SeCN)₂, its crystal structure and physical properties (conductivity, conductivity anisotropy, thermopower and magnetoresistance). The latter are compared to those of its thiocyanate analog (ET)₂TlHg(SCN)₄.

Experimental.

The (ET)₂TlHg(SeCN)₄ crystals were prepared by electrochemical oxidation of ET (2×10^{-3} M) on a Pt anode under galvanostatic regime ($I = 0.8$ A, $j = 0.25$ μ A/cm²) at constant temperature (20 °C). 1, 2-dichloroethane with addition of 10 vol.% absolute ethanol was used as a solvent. The electrolyte was prepared by successive dissolution of 18-crown-6-ether (5×10^{-3} M), TlSeCN (10^{-2} M) and Hg(SeCN)₂ (5×10^{-3} M) in the above mentioned solvent in an electrochemical cell. Initial TlSeCN or Hg(SeCN)₂ salts were prepared by exchange reactions between concentrated water solutions of KSeCN and TlNO₃ or HgCl₂, respectively. Then they were washed with distilled water and absolute ethanol and dried under vacuum.

Experimental X-ray data for 4 063 independent reflections with $I \geq 3 \sigma(I)$ were registered on a diffractometer Syntex P1 with $\theta/2 \theta$ scanning, $(\sin \theta/\lambda)_{\max} = 0.5385$. The structure was solved by a direct method and refined with the least square method in anisotropic-isotropic (for the H atoms) approximation up to $R = 0.031$.

The samples were of different shapes : from lengthened rather thin plates of a hexagonal shape with the typical dimensions of $(1 \times 0.05 \times 0.3)$ mm³ to thick nearly rectangular cubes of $(0.4 \times 0.3 \times 0.4)$ mm³ in size. In almost all samples the crystallographic **a** and **c** axes (in the conducting plane) were directed not along the edges of the crystal but near the sample diagonals and were found by X-ray analysis in each case. The measurement probes were aligned with respect to the crystal axes with an accuracy of approximately $\pm 15^\circ$.

Unfortunately, the small sizes of the samples did not allow a correct determination of the relatively low anisotropy of their conductivity in the **ac** plane. More or less reliable measurements were made for resistivity along the **a** (R_a) and **c** (R_c) axes for one crystal only. In the majority of cases, resistivity along some direction in the **ac** plane (R_{ac}) and perpendicular to it (R_b) was measured for the evaluation of the resistivity anisotropy, ρ_b/ρ_{ac} .

A standard four probe dc- or ac-technique was used for the resistance measurements. The crystals were glued with a graphite paste to four platinum wires of $10 \div 20$ μ m in diameter. Thick short crystals with dimensions of approximately $(0.4 \times 0.3 \times 0.4)$ mm³ were chosen for the R_b measurement. The lengthened thin samples were used for the resistivity measurements

in the ac plane. However, it is evident that at high resistivity anisotropy, ρ_b/ρ_{ac} , the real resistivity along the contact direction in the ac plane, ρ_{ac} , is not equal to the value measured, ρ_{ac}^{meas} , if all four contacts are glued to the same plane of the sample. In this case, the greater part of the current runs near this plane, thus resulting in an increase in the ρ_{ac}^{meas} value. At $\rho_b/\rho_{ac} \geq (\ell_{ac}/\ell_b)^2$, as shown in [15],

$$\rho_{ac}^{\text{meas}} = A \cdot \rho_{ac}, \quad \text{where } A \cong 2 \cdot \frac{\ell_b}{\ell_{ac}} \sqrt{\frac{\rho_b}{\rho_{ac}}}, \quad (1)$$

ℓ_b is the crystal thickness, ℓ_{ac} is the distance between the current contacts, ρ_b is resistivity along b^* . In the present study $R_a(T)$, $R_c(T)$ or $R_{ac}(T)$ dependencies were defined from the measurements of $R_b(T)$ and $R_a^{\text{meas}}(T)$, $R_c^{\text{meas}}(T)$ or $R_{ac}^{\text{meas}}(T)$ ones, respectively, taking into account the correction (1).

The thermopower, S , was measured by an alternating gradient technique according to Chaikin and Kwak [16]. The apparatus was calibrated by measuring 99.99 % pure Pb sample. The single crystals used had the shape of a nearly rectangular thick plate of $(0.6 \times 0.1 \times 0.6) \text{ mm}^3$ dimensions.

The magnetoresistivity perpendicular to the conducting ac plane was measured on one sample in the magnetic fields up to 14 T generated by a superconducting solenoid at temperatures down to 0.35 K. The magnetic field was directed perpendicular to the ac plane.

Results and discussion.

STRUCTURE. — It was established that the radical-cation salt $(\text{ET})_2\text{TIHg}(\text{SeCN})_4$ is isostructural with that of α - $(\text{ET})_2\text{TIHg}(\text{SCN})_4$ [2, 3]. The unit cell parameters of these crystals are listed in table I. The crystals are triclinic with the space group $P\bar{1}$, $Z = 2$.

Table I. — Unit cell parameters for crystals α - $(\text{ET})_2\text{TIHg}(\text{XCN})_4$, where X = S, Se.

Parameter	S	Se
$a, \text{Å}$	10.051(2)	10.105(1)
$b, \text{Å}$	20.549(4)	20.793(3)
$c, \text{Å}$	9.934(2)	10.043(1)
$\alpha, ^\circ$	103.63 (1)	103.51 (1)
$\beta, ^\circ$	90.48 (1)	90.53 (1)
$\gamma, ^\circ$	93.27 (1)	93.27 (1)
$V, \text{Å}^3$	1990(1)	2047.9(8)

Figure 1 represents the projection of the $(\text{ET})_2\text{TIHg}(\text{SeCN})_4$ crystal structure along the c -direction. The structure is characterized with alternation of ET radical-cation and polymer anion layers along the b -axis. The conducting radical-cation layers belong to an α -type packing motif with two crystallographically non-equivalent stacks, A (I, I, I...) and B (II, III, II, III...). The dihedral angles between the radical-cation ET in the neighboring stacks are equal to 105.3° for I-II and 99.8° for I-III, the II-III dihedral angle is 5.7° . In the radical-cation layer there is a large number of shortened interstack contacts S...S (3.495-3.684 Å). However, they are fewer in number and longer than those in the sulfur analog [17].

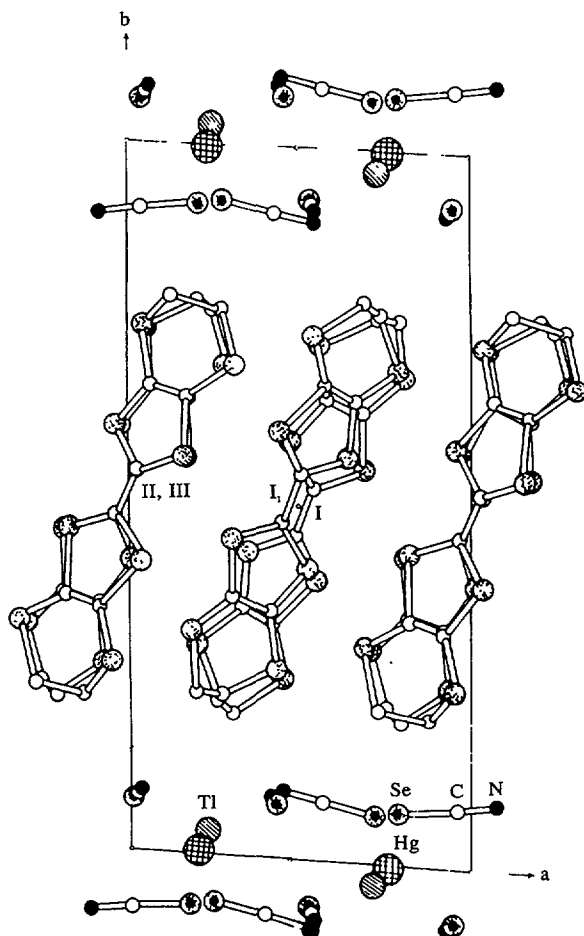


Fig. 1. — Projection of α -(ET)₂TlHg(SeCN)₄ crystal structure along the c-axis.

The anion layer projection along the **b**-direction is shown in figure 2. Each selenocyanate group of the layer is a bridge one between Tl⁻ and Hg²⁺. In this way a polymer net is formed in the **ac**-plane, in which the Hg²⁺ ion has tetrahedral coordination from four Se atoms of the SeCN groups with the Hg-Se interatomic distances of $2.640 \div 2.651(1)$ Å. In accordance with the difference in the covalent radii of the Se and S atoms these distances are ≈ 0.1 Å longer than those of Hg-S in α -(ET)₂MHg(SCN)₄ with M = Tl [2, 3], K [18, 19], NH₄ [19] and Rb [20]. The Tl⁻ ion has a typical coordination, in which four short bonds are located to one side, while four much elongated secondary bonds are on the other side [21]. The Tl⁻ ion is at the top of the pyramid and is bound to four N atoms of the SeCN groups, the interatomic Tl-N distances are $2.988 \div 3.010(10)$ Å, the corresponding values in the sulfur analog being equal to $2.935 \div 3.019(8)$ Å [2]. Four Tl.. Se bonds of $3.456 \div 3.616(1)$ Å add to the Tl⁻ coordination up to 8 (a tetragonal antiprism).

A detailed comparison of the (ET)₂TlHg(SeCN)₄ structure with that of (ET)₂TlHg(SCN)₄ showed them to have the same architecture of the conducting layer without any orientation disorder characteristic of the other ET-based organic metals. However, it should be noted that while, in the sulfur analog, three crystallographically independent ET are similar in the

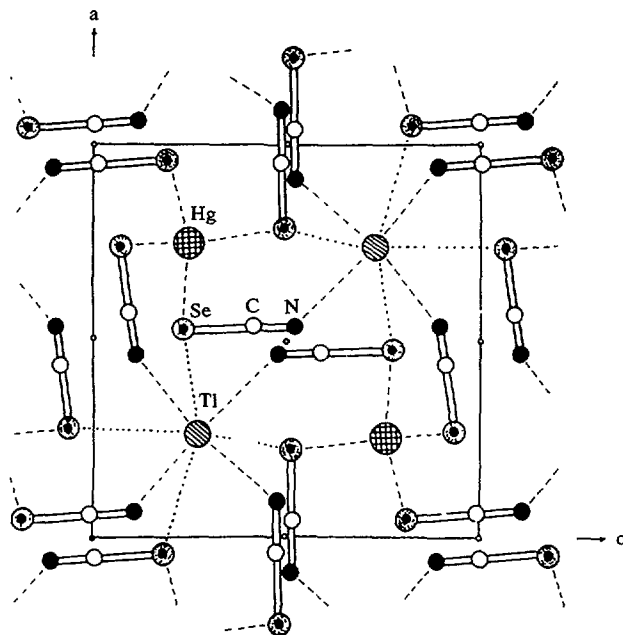


Fig. 2. — Projection of α - $(\text{ET})_2\text{TlHg}(\text{SeCN})_4$ anion layer along the \mathbf{b} -axis.

character of the bond length distribution corresponding to $\text{ET}^{0.5+}$ (like in crystals with $\text{M} = \text{K}$ and NH_4 [18, 19]), it is not so in the selenium analog. Thus, the central bond length $\text{C}=\text{C}$ for ET in general position is equal to $1.39(1) \text{ \AA}$, which is close to ET^+ , while for two centrosymmetric ET it is equal to $1.33(1) \text{ \AA}$, which is closer to the value in the neutral ET^0 molecule.

The result stated above can be evidence for some charge localization in the radical-cation layer at room temperature. If such a character of the bond length distribution remains at low temperatures, it could be the explanation of the fact that although α - $(\text{ET})_2\text{TlHg}(\text{SeCN})_4$ is an organic metal stable down to the lowest temperatures (like α - $(\text{ET})_2\text{NH}_4\text{Hg}(\text{SCN})_4$, it does not undergo a superconducting transition (unlike the latter).

RESISTIVITY. — The temperature dependencies of resistance along the \mathbf{a} , \mathbf{c} , and \mathbf{b}^* axes are plotted in figure 3 for the same $(\text{ET})_2\text{TlHg}(\text{SeCN})_4$ single crystal. It should be noted that the $R_a(T)/R(295)$ curve of this sample is located somewhat higher than that of $R_c(T)/R(295)$ in contrast to the $(\text{ET})_2\text{TlHg}(\text{SCN})_4$ samples [2]. The $R_b(T)/R(295)$ curves for the Se- and S-samples are always situated higher than those of $R(T)/R(295)$ for any direction in the \mathbf{ac} plane, the ratio $R(295)/R(1.3)$ and the curvature of the $R(T)/R(295)$ dependencies may vary when going from one sample to another.

The low-temperature parts of the $R(T)/R(12)$ dependencies for various directions and different α - $(\text{ET})_2\text{TlHg}(\text{SeCN})_4$ crystals are shown in figure 4. Both R_{ac} and R_b are seen either to be practically constant below $\approx 4 \text{ K}$ or to diminish slowly down to $\approx 2 \div 3 \text{ K}$. With lowering temperature, the tendency is observed to some resistance growth, which can be caused by localization effects. No traces of superconductivity have been detected down to 0.3 K .

The values of room conductivity in the \mathbf{ac} plane with the account of correction (1) are equal to $\sigma_a \approx 140 \text{ Ohm}^{-1} \text{ cm}^{-1}$ and $\sigma_c \approx 24 \text{ Ohm}^{-1} \text{ cm}^{-1}$ for the same crystal, while the measured

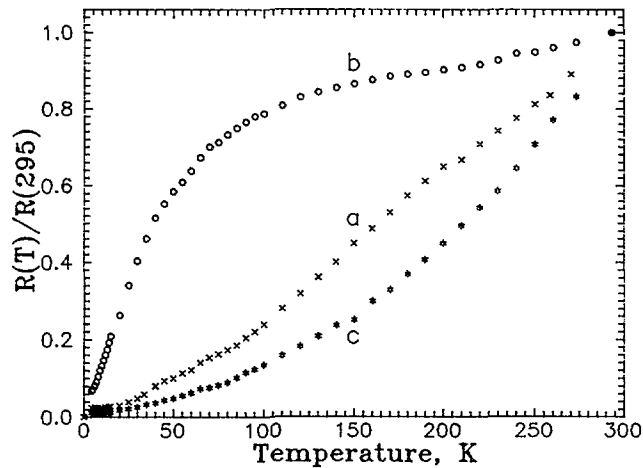


Fig. 3. — Temperature dependence of resistance for the same α -(ET) $_2$ TIHg(SeCN) $_4$ crystal along different crystallographic directions : a) along the **a**-axis, b) along the **b***-direction, c) along the **c**-axis.

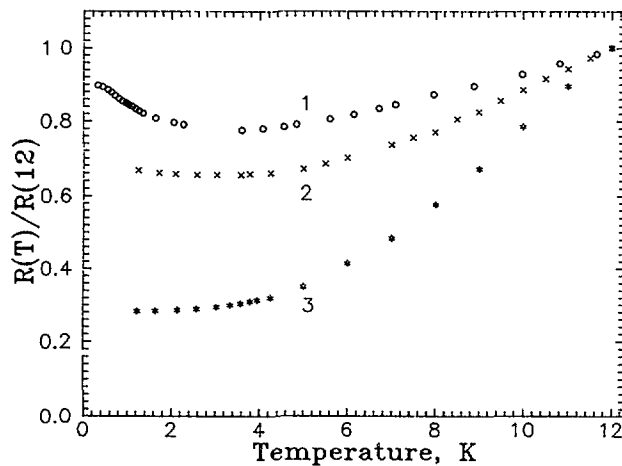


Fig. 4. — Low-temperature dependencies of the resistance for different crystals of α -(ET) $_2$ TIHg(SeCN) $_4$ along different crystallographic directions : 1) and 3) along the **b***-direction, 2) along some direction in **ac**-plane.

values were an order of magnitude lower. The conductivity in the direction perpendicular to the **ac** plane (σ_b) ranges in various crystals from 4×10^{-4} to 7×10^{-3} Ohm $^{-1}$ cm $^{-1}$. Thus, at room temperature the resistance anisotropy of the Se crystals is equal to $\rho_a \cdot \rho_c / \rho_b = 1.6 : (2 \div 35) \times 10^4$.

The temperature dependencies of the ρ_b/ρ_a , ρ_b/ρ_c and ρ_c/ρ_a anisotropies are shown in figure 5 for the same crystal as in figure 3. The $\rho_b/\rho_a(T)$ and $\rho_b/\rho_c(T)$ dependencies are seen to be similar. The anisotropy increases approximately by an order of magnitude with decreasing temperature down to 30 K and then it is reduced by ≈ 2 times to helium temperatures. At the same time, the ratio ρ_c/ρ_a exhibits essentially a monotonous ≈ 3 -fold decrease.

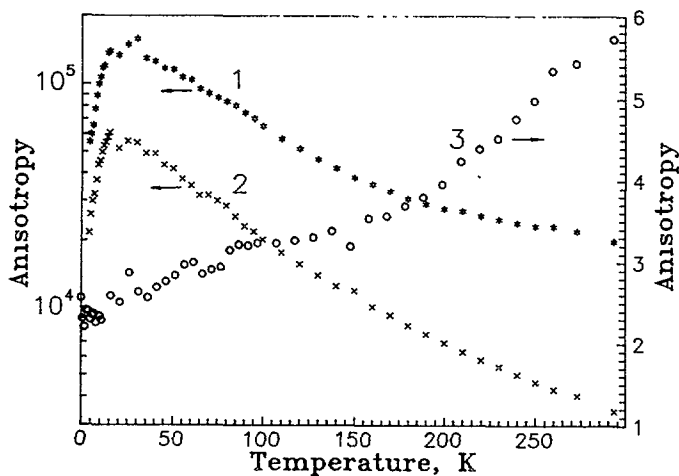


Fig. 5. — Temperature dependence of the resistance anisotropy for the same crystal as in figure 3 : 1) ρ_b/ρ_a , 2) ρ_b/ρ_c , 3) ρ_c/ρ_a .

The fact that shortened interstack S ... S contacts are longer and less numerous in the Se crystals than in their S analogs must result in less resistance anisotropy in the conducting plane. Indeed, the ρ_c/ρ_a for the Se crystals is lower than that for the sulfur analogs [2]. A thicker anion layer in the Se crystals (due to the difference in the covalent radii of the Se and S atoms) conditions a higher resistivity along the direction perpendicular to the conducting layers and consequently the greater value of the ρ_b/ρ_a anisotropy for the Se samples. These data confirm an earlier supposition [22] of an extremely weak corrugation of the Fermi cylinder in α -(ET)₂TIHg(SeCN)₄. The above described peculiarities of the structure of this compound are likely to be also the cause of different temperature dependencies of the ρ_b/ρ_c and the ρ_c/ρ_a in the Se and S salts (Fig. 5 and [2], respectively).

MAGNETORESISTANCE. — Figure 6 shows the dependence of the magnetoresistance, MR, on the magnetic field directed perpendicular to the *ac* plane at $T = 0.35$ K. The classical part of MR grows gradually with increasing field and tends to saturate at a constant value, $\Delta R(H)/R(0) \approx 0.5$ in fields above 10 T. Clear Shubnikov-de-Haas (SdH) oscillations become visible starting from ≈ 4 T. No splitting of the oscillations was found up to 14 T. As seen in the inset in figure 6, the Fourier transformation reveals the fundamental frequency $F_0 = (665 \pm 5)$ T and only a small second harmonic, $F_2 = (1\,330 \pm 5)$ T, with an amplitude not exceeding a few percent of the fundamental. The cyclotron mass determined from the temperature dependence of the oscillation amplitude is $m_c = (2.05 \pm 0.05)m_e$, where m_e is the free electron mass. More detailed data on the SdH oscillations as well as the MR anisotropy are published elsewhere [22].

The MR behavior is very much like that in the isostructural α -(ET)₂NH₄Hg(SCN)₄ salt [23] and is drastically different from those in the α -(ET)₂MHg(SCN)₄ salts with M = K [24, 25] and TI [10, 26] in their low-temperature state. This fact shows that all the anomalies found in the latter compounds, such as giant MR, high-field kink structure, splitting of the SdH oscillations etc. [3, 4, 6-8, 10-12, 26], are associated inherently with the specifics of their low-temperature electronic state as discussed in detail in [10, 12].

We would like to emphasize that the cyclotron mass, $m_c \approx 2m_e$, obtained from the SdH oscillations is very close to that in the NH₄(SCN) salt [23] and about 1.5 times larger than

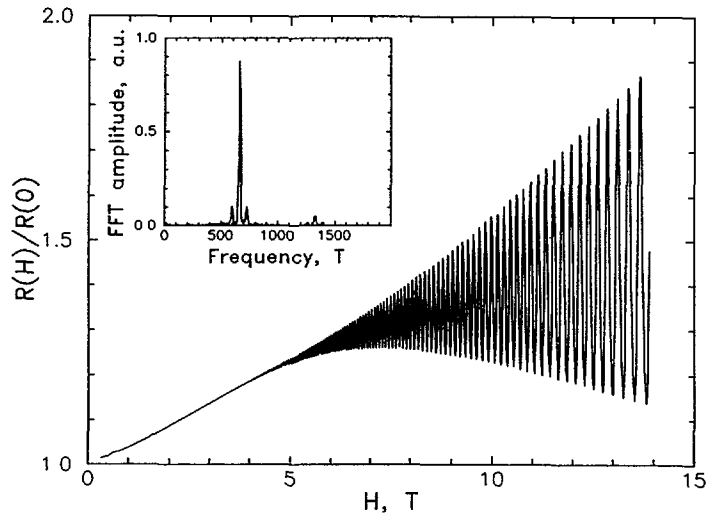


Fig. 6. — Dependence of the magnetoresistance on the magnetic field perpendicular to the *ac*-plane, $T = 0.35$ K. The inset shows the Fourier spectrum of SdH oscillations.

m_c in Tl-(SCN) [26] and K-(SCN) [24, 25]. Meanwhile, taking into account the closeness of the crystal parameters of the α -(ET)₂MHg(SCN)₄ salts, the band structure calculations are expected to give approximately the same band mass values, m_b , for all of them. Since the amplitude of the SdH oscillations is determined by the cyclotron mass renormalized by many-body interactions, $m_c = m_b(1 + \lambda)$, where λ is the function of electron-phonon and electron-electron interactions [27], the significant difference between m_c in the « normal-state » Tl-(SeCN) and NH₄-(SCN) salts and that in the low-temperature state of Tl-(SCN) and K-(SCN) may be an evidence for the essential role of many-body correlations in these systems.

THERMOPOWER. — Figure 7 shows temperature dependencies of the thermopower, $S(T)$, along the *a*-, *c*- and *b**-directions for one of the α -(ET)₂TIHg(SeCN)₄ samples. Three characteristic features in the data should be noted.

1) For the *c*-direction, S_c is positive in the whole range from the room temperature to 4.2 K. The samples show flattening of the $S(T)$ curve common for the α -(ET)₂MHg(SCN)₄ compounds at high temperatures.

2) For the *a*-direction, the thermopower of the samples, which is positive at room temperature, changes its sign at 210 K and shows a broad minimum at about 150 K tending to zero at further cooling.

3) For the *b**-direction, S is positive at all temperatures and decreases approximately linearly with lowering temperature.

The thermopower behavior appears to be consistent with the coexistence of an open electron Fermi surface (FS) sheet and a closed hole one predicted by the band structure calculation for the α -(ET)₂MHg(SCN)₄ compounds [28]. In the *c*-direction the transport is dominated by the holes from the FS cylinders. Thus we may estimate the Fermi energy, ε_F , for the hole band from the general formula, valid for the one-band transport :

$$S = \frac{\pi^2 k^2 T}{3 e \varepsilon_F} \left(\frac{\partial \ln \sigma(\varepsilon)}{\partial \ln \varepsilon} \right)_{\varepsilon_F}, \quad (2)$$

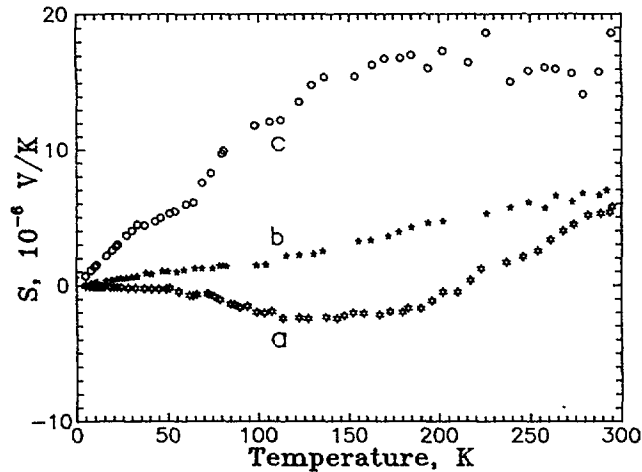


Fig. 7. — Thermopower vs. temperature dependencies : a) along the a-axis, b) along the b^* -direction, c) along the c-axis.

where $\sigma(\varepsilon)$ is an energy dependent conductivity. Assuming the scattering term in parentheses to be equal to unity we get, from the experimentally obtained slope of the $S_c(T)$ curve, $0.9 \times 10^{-7} \text{ V/K}^2$, ε_F for the hole band of approximately 0.3 eV.

As follows from the band structure calculation, the carriers from both the open electron sheet and the hole cylinder may contribute to S_a . However, compared to $(\text{ET})_2\text{TIHg}(\text{SeCN})_4$, $S_a(T)$ in $(\text{ET})_2\text{TIHg}(\text{SeCN})_4$ is considerably shifted upward, to positive thermopower values. That is why we may conclude that the hole contribution is higher in $(\text{ET})_2\text{TIHg}(\text{SeCN})_4$ than in $(\text{ET})_2\text{TIHg}(\text{SCN})_4$. Meanwhile, the cross section areas of the FS hole cylinders for both compounds determined from magnetoresistance oscillations [3, 22] are close to each other. In view of the same structures and very close crystal parameters of the compounds it is natural to expect approximately the same volume of the electron FS part. Therefore the larger hole contribution to the thermopower in $(\text{ET})_2\text{TIHg}(\text{SeCN})_4$ may be due to the hole mobility increase. The latter is likely supported by the essential increase of the SdH oscillation amplitude [22].

It is worth noting that vanishing of thermopower in the $(\text{ET})_2\text{TIHg}(\text{SCN})_4$ salt at the phase transition temperature, 10 K [29], has not been observed in $(\text{ET})_2\text{TIHg}(\text{SeCN})_4$ in accordance with the conductivity results (Fig. 4).

The $S_b(T)$ dependencies are approximately linear in temperature. This behavior is usually observed in other two-dimensional organic conductors [30] and high- T_c superconductors [31, 32].

Conclusion.

An ET salt with a metal complex anion containing a selenocyanate ligand, α - $(\text{ET})_2\text{TIHg}(\text{SeCN})_4$, has been synthesized. This compound has been found to be isostructural to sulfur analogs α - $(\text{ET})_2\text{MHg}(\text{SCN})_4$, where $M = \text{K}, \text{Tl}, \text{NH}_4$ and Rb . However, a low-temperature phase transition characteristic of the α - $(\text{ET})_2\text{MHg}(\text{SCN})_4$ with $M = \text{K}, \text{Tl}$ and Rb has not been revealed by conductivity, magnetoresistance and thermopower measurements in α - $(\text{ET})_2\text{TIHg}(\text{SeCN})_4$ as well as in α - $(\text{ET})_2\text{NHg}(\text{SCN})_4$. But in contrast to the NH_4 -salt, a superconducting transition in α - $(\text{ET})_2\text{TIHg}(\text{SeCN})_4$ is not observed down to 0.3 K.

A detailed structural analysis shows that, unlike in its S-analogs, all three crystallographically independent ET molecules in the Se-salt differ from each other in the distribution of their bond lengths; this might lead to charge localization effects in the cation layers. The resistivity anisotropy is shown to be lower in the ac-plane and higher in the perpendicular planes than in the S-salt. This is in accordance with the thicker anion layers and smaller number of shortened interstack S ... S contacts in the compound studied.

The observed SdH oscillations reveal a cylindrical FS consistent with that predicted by the band structure calculation [28]. The comparison of the MR and thermopower in the present compound with those in α -(ET)₂MHg(SCN)₂ with M = K and Tl shows that all the MR anomalies as well as vanishing thermopower below 10 K found in the latter compounds are inherently relevant to their specific low-temperature state.

Acknowledgements.

We are thankful to Prof. I. F. Schegolev for his interest and encouragement. The work was supported by the Science Council on HTSC problem and carried out in the framework of the project No. 90346 of the State Program « High-temperature superconductivity ». This work was also supported, in part, by a Soros Foundation Grant awarded by the American Physical Society.

References

- [1] Wang H. H., Carlson K. D., Geiser U., Kwok W. K., Vashon M. D., Thompson J. E., Larsen N. F., McCabe G. D., Hulscher R. S. and Williams J. M., *Physica C* **166** (1990) 57.
- [2] Schegolev A. I., Laukhin V. N., Khomenko A. G., Kartsovnik M. V., Shibaeva R. P., Rozenberg L. P. and Kovalev A. E., *J. Phys. I France* **2** (1992) 2123.
- [3] Kushch N. D., Buravov L. I., Kartsovnik M. V., Laukhin V. N., Pesotskii S. I., Shibaeva R. P., Rozenberg L. P., Yagubskii E. B. and Zvarykina A. V., *Synth. Met.* **46** (1992) 271.
- [4] Sasaki T., Toyota N., Tokumoto M., Kinoshita N. and Anzai H., *Solid State Commun.* **75** (1990) 93.
- [5] Kinoshita N., Tokumoto M. and Anzai H., *J. Phys. Soc. Jpn* **60** (1991) 2131.
- [6] Sasaki T., Sato H. and Toyota N., *Synth. Met.* **41-43** (1991) 2211.
- [7] Tokumoto M., Swanson A. G., Brooks J. S., Agosta C. C., Hannahs S. T., Kinoshita N., Anzai H. and Anderson J. R., *J. Phys. Soc. Jpn* **59** (1990) 2324.
- [8] Osada T., Yagi R., Kawasumi A., Kagoshima S., Miura N., Oshima M. and Saito G., *Phys. Rev. B* **41** (1990) 5428.
- [9] Kartsovnik M. V., Kovalev A. E., Laukhin V. N., Pesotskii S. I. and Kushch N. D., *Pis'ma v Zh. Eksp. Teor. Fiz.* **55** (1992) 337 [*JETP Lett.* **55** (1992) 339].
- [10] Kartsovnik M. V., Kovalev A. E. and Kushch N. D., *J. Phys. I France* **3** (1993) 1187.
- [11] Pratt F. L., Singleton J., Doperto M., Fisher A. J., Janssen T. J. B. M., Perenboom J. A. A. J., Kurmoo M., Hayes W. and Day P., *Phys. Rev. B* **45** (1992) 13904.
- [12] Kartsovnik M. V., Mashovets D. V., Smirnov D. V., Laukhin V. N., Gilewski A. and Kushch N. D., submitted to *J. Phys. I France*.
- [13] Ito H., Kaneko H., Ishiguro T., Ishimoto H., Kono K., Horuchi S., Komatsu T. and Saito G., *Solid State Commun.* **85** (1993) 1005.
- [14] Mori H., Tanaka S., Oshima K., Saito G., Mori T., Maruyama Y. and Inokuchi H., *Synth. Met.* **41-43** (1991) 2013.
- [15] Buranov L. I., to be published.
- [16] Chaikin P. M. and Kwak J. F., *Rev. Sci. Instr.* **46** (1975) 218.
- [17] Shibaeva R. P., Rozenberg L. P., Kushch N. D. and Yagubskii E. B., *Kristallografija* (in press).
- [18] Oshima M., Mori H., Saito G. and Oshima K., *Chem. Lett.* (1989) 1159.

- [19] Mori H., Tanaka S., Oshima M., Saito G., Mori T., Maruyama Y. and Inokuchi H., *Bull. Chem. Soc. Jpn* **63** (1990) 2183.
- [20] Mori H., Tanaka S., Oshima K., Saito G., Mori T., Maruyama Y. and Inokuchi H., *Synth. Met.* **41-43** (1991) 2013.
- [21] Wells A. F., *Structural inorganic chemistry*. M. « Mir » V.3 (1987) p. 315.
- [22] Kovalev A. E., Kartsovnik M. V. and Kushch N. D., *Solid State Commun.* **87** (1993) 705.
- [23] Osada T., Kawasumi A., Yagi R., Kagoshima S., Miura N., Oshima M., Mori H., Nakamura T. and Saito G., *Solid State Commun.* **75** (1990) 901.
- [24] Osada T., Yagi R., Kawasumi A., Kagoshima S., Miura N., Oshima M. and Saito G., *Phys. Rev. B* **41** (1990) 5428.
- [25] Sasaki T., Toyota N., Tokumoto M., Kinoshita N. and Anzai H., *Solid State Commun.* **75** (1990) 97.
- [26] Kartsovnik M. V., Kovalev A. E., Laukhin V. N. and Pesotskii S. I., *J. Phys. I France* **2** (1992) 223.
- [27] Shoenberg D., *Magnetic oscillations in metals* (Cambridge University Press, Cambridge, 1984).
- [28] Mori T., Inokuchi H., Mori H., Tanaka S., Oshima M. and Saito G., *J. Phys. Soc. Jpn* **59** (1990) 2624.
- [29] Tanatar M. A., Yefanov V. S., Dyakin V. V., Bondarenko V. A., Kushch N. D. and Yagubskii E. B., *Synt. Met.* **56/1** (1993) 2419.
- [30] Bondarenko V. A., Dyakin V. V., Yefanov V. S., Tanatar M. A., Kushch N. D. and Yagubskii E. B., *Synt. Met.* **56/1** (1993) 2391.
- [31] Ma H., Xiong G., Wang L., Wang S., Zhang H., Tong L., Liang S. and Yan S., *Phys. Rev. B* **40** (1989) 9374.
- [32] Geim A. K. and Dubonos S. V., *Sverkhprovodimost'* **2** (1989) 5.